

## Supersymmetric Higgs Bosons in Weak Boson Fusion

Wolfgang Hollik,<sup>1</sup> Tilman Plehn,<sup>2</sup> Michael Rauch,<sup>2</sup> and Heidi Rzehak<sup>3</sup><sup>1</sup>*Max-Planck-Institut für Physik (Werner-Heisenberg-Institut), Munich, Germany*<sup>2</sup>*SUPA, School of Physics, University of Edinburgh, Scotland*<sup>3</sup>*Paul Scherrer Institut, Villigen PSI, Switzerland*

We compute the complete supersymmetric next-to-leading order corrections to the production of a light Higgs boson in weak boson fusion. The size of the electroweak corrections is of similar order as the next-to-leading order corrections in the Standard Model. The supersymmetric QCD corrections turn out to be significantly smaller than their electroweak counterparts. These higher-order corrections are an important ingredient to a precision analysis of the (supersymmetric) Higgs sector at the LHC, either as a known correction factor or as a contribution to the theory error.

PACS numbers: 14.80.Cp, 13.85.Qk

The main task of the LHC era is to understand electroweak symmetry breaking and the ultraviolet completion of the Standard Model. According to electroweak precision data we expect to see a light Higgs boson, which should be embedded into a UV completion solving the hierarchy problem. A minimal realization of TeV-scale supersymmetry (MSSM) is a leading candidate for that. The most promising discovery channel for a light supersymmetric Higgs boson is the production in weak-boson fusion with a subsequent decay into tau leptons [1, 2]. There, a light supersymmetric Higgs scalar is guaranteed to appear over the entire MSSM parameter space [3].

In the Standard Model as well as in the MSSM, many years of LHC running will be devoted to understanding the Higgs sector in detail, for example extracting the gauge and Yukawa couplings [4]. To meaningfully distinguish between, for example, the Standard-Model and the MSSM Higgs sectors [5] we need to control the theory error on the LHC rates including higher-order effects. In the Standard Model the next-to-leading order QCD and electroweak corrections to weak-boson-fusion Higgs production are known to be fairly small [6]. In particular, the QCD corrections are suppressed due to the color structure of the production process and the forward-jet topology. Also interference effects between Higgs production in weak-boson fusion and in gluon fusion with two additional jets are strongly suppressed [7].

For either a comparison between the Standard-Model and the MSSM Higgs sectors or for a precision analysis of the MSSM Higgs sector these higher-order corrections have to be augmented by supersymmetric particle loops. In parallel to the Higgs searches, the LHC experiments will also search for direct signatures of new physics. If we should find such new states we can then predict their effects on the Higgs sector. If, for example, squarks and gluinos should be too heavy or the spectrum should be not favorable to precision MSSM analyses [8], we need to include their effects in the theory errors. Both cases require a comprehensive calculation of the supersymmetric contributions to the weak-boson-fusion and gluon-fusion production processes [9].

Supersymmetry vs Standard Model — Compared to its Standard-Model counter part the leading-order production rate of a light supersymmetric Higgs scalar  $h^0$  includes an additional coupling factor  $\sin(\beta - \alpha)$ . It is expressed in terms of the ratio of the vacuum expectation values  $\tan\beta$  and the scalar mixing angle  $\alpha$  from the supersymmetric two-Higgs-doublet model. For a given Higgs mass we can relate the tree-level MSSM production rate to the Standard-Model result via a simple re-scaling by  $\sin^2(\beta - \alpha)$ . For large pseudoscalar Higgs masses  $m_A \gtrsim 200$  GeV this factor is very close to unity.

Including higher orders, there are additional contributions from the supersymmetric particle spectrum: first, we take into account loops of supersymmetric partners. If we assume  $R$  parity, one-loop diagrams cannot mix supersymmetric and Standard-Model particles, allowing for a diagram-by-diagram separation of the MSSM contributions. Secondly, the additional supersymmetric Higgs bosons with their Standard-Model type  $R$  charge appear in loops. Because the Standard-Model Higgs boson does not simply correspond to one supersymmetric Higgs boson we cannot separate the Standard-Model Feynman diagrams from the MSSM set. Instead, we first compute the MSSM-Higgs corrections and then subtract the Standard-Model Higgs loops, scaled by the tree-level correction factor.

Because of the large number of Feynman diagrams we compute the cross sections using the automated tool HadCalc [10]. The Feynman diagrams and the amplitudes we generate with FeynArts/FormCalc [11]. The loop integrals we evaluate using LoopTools [12]. We assume minimal flavor violation, because after taking into account all experimental and theoretical constraints, the effect of non-minimal flavor violation on LHC rates is small [13]. We also assume a  $CP$ -conserving MSSM.

Higgs-sector corrections — The mass of the light supersymmetric Higgs boson  $m_h$  is not a free parameter. At tree level it can be computed from  $m_A$  and  $\tan\beta$  and is always smaller than  $m_Z$ . Higher-order corrections, dominated by the top Yukawa coupling term  $h_t^4$

	effective theory		Feynman diagrams	
	$\alpha_{\text{eff}}$	full	$\alpha_{\text{eff}}$	full
$\lambda_{HHH}$	0.208	0.198	0.210	0.210
$\lambda_{HHh}$	-0.285	-0.275	-0.284	-0.279
$\lambda_{Hhh}$	-0.216	-0.219	-0.220	-0.257
$\lambda_{hhh}$	0.952	1.503	0.950	1.276
$\alpha_{\text{eff}}$	-0.1132		-0.1158	
$m_h$	109.8 GeV		111.0 GeV	
$m_H$	391.5 GeV		391.6 GeV	

Table I: Higgs self couplings for the parameter point SPS1a following Ref. [17] (left) and Ref. [15] (right). The common factor  $-3em_W/(2c_W^2sw)$  is not included.

at one-loop order, push  $m_h$  to values beyond the LEP2 limits [14, 15, 16, 17, 18]. Phenomenologically relevant studies therefore need to include quantum corrections to the Higgs mass and the Higgs potential.

The challenge in including these higher-order corrections in our calculation is that we cannot simply shift the final-state Higgs mass. Already in the Standard Model the physical Higgs mass  $m_h$  is linked to the running quartic coupling  $\lambda(Q)$  and top Yukawa  $h_t(Q)$  [19]

$$\frac{m_h^2}{\lambda(Q)v^2} = 1 - \frac{3h_t^2(Q)}{16\pi^2} \left[ Z \left( \frac{4m_t^2}{m_h^2} - 1 \right) - 2 \right] \left[ 1 - \frac{4m_t^2}{m_h^2} \right] - \frac{3h_t^2(Q)}{16\pi^2} \left[ 2 - \frac{4m_t^2}{m_h^2} \right] \log \frac{Q^2}{m_t^2} \quad (1)$$

with  $Z(x) = 2\sqrt{x} \tan^{-1}(x^{-1/2})$  for  $x > 1/4$ . When including self-energy corrections to the Higgs mass, we should also correct the Higgs self couplings at the same order in perturbation theory. While this has to be done explicitly [20] in a Feynman-diagrammatic approach [14, 15] it is automatically taken care of if we compute the quantum effects in the scalar potential [16, 17].

On the other hand, quantum corrections to the Higgs potential are usually computed for vanishing external momentum instead of  $p^2 = m_h^2$ . In the Feynman-diagrammatic approach it is straight forward to compute the Higgs self-energy diagrams with a finite momentum flow, while this is a challenge for the effective-potential method.

Last but not least, when computing the effective scalar potential using renormalization-group techniques, it becomes increasingly tedious to separate scales, like the heavy Higgs mass  $m_A$ , the light stop mass  $m_{\tilde{t}_1}$  and the gluino mass  $m_{\tilde{g}}$ .

Because the light supersymmetric Higgs boson is the lightest particle in the supersymmetric loops we expect the numerical effects of its mass and of the associated self coupling  $\lambda_{hhh}$  to be non-negligible. In Tab. I we compare the values for the scalar self couplings in the effective theory approach (implemented from Ref. [17]) with those from the Feynman-diagrammatic FeynHiggs package [15]. Both approaches allow for an approximate computation introducing an effective mixing angle  $\alpha_{\text{eff}}$  from the scalar

$ \Delta\sigma/\sigma(ud \rightarrow udh)  (\sigma_{\alpha_{\text{eff}}} - \sigma_{\text{full}})/\sigma$		
effective theory		
$\alpha_{\text{eff}}$	-0.389 %	-0.122 %
full	-0.266 %	
Feynman diagrams		
$\alpha_{\text{eff}}$	-0.393 %	-0.076 %
full	-0.317 %	
Feynman diagrams, loop-improved $Z_{\text{FH}}$		
$\alpha_{\text{eff}}$	-0.343 %	-0.115 %
full	-0.228 %	

Table II: Schemes for computing the supersymmetric corrections to the  $VVh$  vertices at the hadronic level, for the leading partonic subprocess.

Higgs mass matrix. In this case the trilinear Higgs coupling  $\lambda_{hhh}$  is given by the Standard-Model coupling times the MSSM correction factor  $\cos 2\alpha_{\text{eff}} \sin(\beta + \alpha_{\text{eff}})$ . The results in this approximation should be equivalent in both schemes, because finite values of  $p^2$  as well as corrections to the self couplings are skipped. In Tab. I we see that the  $\alpha_{\text{eff}}$  approximations indeed agree very well. Between the full results, where FeynHiggs includes the fixed-order one-loop  $\mathcal{O}(h_t^4)$  corrections to  $\lambda_{hhh}$  [20], we see the expected small deviations.

For LHC cross sections this comparison is complicated by the different final-state Higgs masses in the two schemes. The effect of all supersymmetric corrections to the  $VVh$  vertices ( $V = W, Z$ ) and the Higgs wavefunction renormalization for the dominant partonic subprocess  $ud \rightarrow udh$  we show in Tab. II. The contributions from the Higgs sector and from supersymmetric particles cannot be separated because of their combined renormalization. The first four lines use a wave-function renormalization at one loop. In the  $\alpha_{\text{eff}}$  approximation the corrections agree well, despite the different external Higgs masses. For the bottom lines we include the higher-order improved wave-function renormalization factors provided by FeynHiggs.

For the numerical analysis in this letter we use the Feynman-diagrammatic approach with one-loop  $Z$  factors, to allow for a proper renormalization-scale behavior. The difference of  $\sim 0.05$  % between the different rate predictions is a lower limit on the remaining theory error from the MSSM Higgs sector. Note, however, that this theory error only applies if we strictly assume the minimal renormalizable supersymmetric Higgs sector.

Supersymmetric particle corrections — Example one-loop diagrams appearing in the  $qq \rightarrow qqh$  processes we show in Fig. 1. Our numerical results are based around the parameter point SPS1a [21], for which there are two aspects we need to remember: supersymmetric particles with only electroweak charges have typical masses of 100–200 GeV, while squarks and gluinos range around 500–600 GeV, and  $\tan\beta = 10$  avoids large non-decoupling effects from down-type fermions.

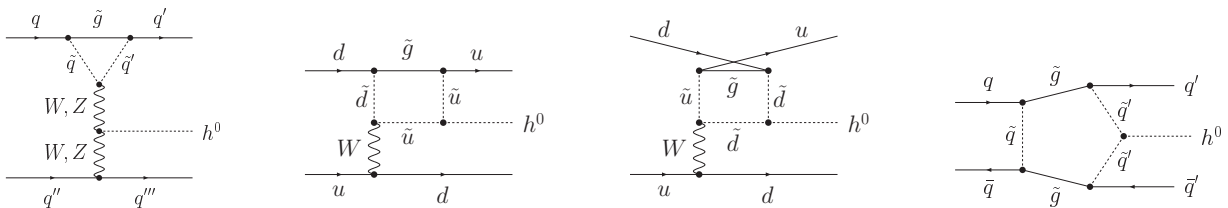


Figure 1: Left to right: Feynman diagrams contributing to strong vertex corrections, strong boxes, strong pentagons.

As we can see in Tab. III all QCD corrections  $\Delta\sigma \propto \alpha^3\alpha_s$  turn out to be surprisingly small. In the Standard Model we know that from a QCD perspective we are essentially looking at two-sided non-interfering deep inelastic scattering. However, there are several mechanisms responsible for an even larger suppression in the supersymmetric case.

Two tree-level vertices receive one-loop corrections,  $qqV$  and  $VVh$ , but only the first is corrected by squark/gluino loops. The  $\tilde{q}\tilde{q}'W$  coupling connects left-handed sfermions. Since the mixing between left and right-handed light-flavor squarks is proportional to the negligible quark Yukawa coupling, both external quarks are then left-handed, just as at tree level. This means that in the one-loop diagram (when closed with the Born diagram) the left-handed fermion trace cannot be connected through a gluino-mass insertion, because this would require a chirality flip. Instead of  $m_{\tilde{g}}$ , the typical momentum scale in the numerator is  $\sim m_h/2$ , an order of magnitude below the gluino mass in the denominator.

In the electroweak case, also the (typically lighter) charginos and neutralinos in the loop couple to the vector boson. This means that we can add a double mass insertion into the fermion line which can partly compensate for the heavy masses in the loop denominator. This effect leads to a relative enhancement of the electroweak over the QCD  $qqV$  vertex correction we observe in Tab. III.

For strongly interacting boxes, the  $\tilde{q}\tilde{q}'W$  and  $q\tilde{q}\tilde{g}$  couplings are the same for both diagrams shown in Fig. 1, but the  $\tilde{q}\tilde{q}h$  coupling is proportional to  $T_3 - Qs_w^2$ , i.e. around  $-1/3$  for down squarks and  $+5/16$  for up squarks. This leads to a cancellation by one order of magnitude,

diagram	$\Delta\sigma/\sigma$ [%]	diagram	$\Delta\sigma/\sigma$ [%]
	$\Delta\sigma \sim \mathcal{O}(\alpha)$		$\Delta\sigma \sim \mathcal{O}(\alpha_s)$
self energies	0.199		
$qqW + qqZ$	-0.392	$qqW + qqZ$	-0.0148
$qqh$	-0.0260	$qqh$	0.00545
$WW h + ZZ h$	-0.329		
box	0.0785	box	-0.00518
pentagon	0.000522	pentagon	-0.000308
sum of all $\Delta\sigma/\sigma = -0.484$ %			

Table III: Complete supersymmetric corrections to the process  $pp \rightarrow qqh$  by diagrams. Our parameter point SPS1a has a tree-level rate of 706 fb.

which could only be broken by different squark masses. Left-handed squarks, however, form a  $SU(2)$  doublet and are governed by the same soft-breaking terms, and the left-right mixing is negligible for light-flavor squarks. This argument does not hold for the sub-leading  $ZZ$  fusion, where we indeed find that the corrections turn out to be at a more natural level.

In the Standard Model the color factor of a gluon exchange between the two incoming quarks is proportional to the trace of the  $SU(3)$  generators and hence zero. The same is true for a pentagon gluino exchange between the incoming quarks, where the color trace is evaluated along quark/squark lines. In Fig. 1, we show another supersymmetric pentagon diagram with a squark exchange between the two incoming quarks. The  $VV$ -fusion is replaced by a squark coupling to the Higgs, which gets rid of the color suppression. Such diagrams contribute formally at order  $\mathcal{O}(\alpha_s^2\alpha^2)$ , which is as large as the Born term  $\mathcal{O}(\alpha^3)$ . However, their kinematic properties are completely different from the vector-boson-fusion topology and the large loop masses further reduce their contribution to an altogether negligible level.

Following all the above arguments the supersymmetric QCD corrections to weak-boson-fusion Higgs production are suppressed by a whole list of mechanisms, which explain their at first sight surprising suppression even with respect to the electroweak corrections in Tab. III.

Looking beyond SPS1a, we show the next-to-leading order corrections for the complete set of SPS parameter points [21] in Tab. IV. From the discussion above we do not expect the picture of electroweak vs. strong corrections to change significantly for any of them. Heavier supersymmetric spectra and different values of  $\tan\beta$  and of the trilinear couplings just scale the over-all size of the supersymmetric corrections. The relatively large corrections for the SPS5 parameter point are driven by a light top squark, while the largely decoupled spectrum in SPS9 leads to negligible MSSM effects. The typical size of the complete MSSM corrections is less or around 1 %.

To study the behavior of the one-loop corrections with varying supersymmetric masses we start from the parameter point SPS1b and run the universal gaugino mass  $m_{1/2}$  from 100 to 1000 GeV. In Fig. 2 we show the result for a  $m_{1/2}$ -dependent Higgsino mass parameter as well as for the fixed SPS1b value  $\mu = 499$  GeV. The

	$\Delta\sigma/\sigma$ [%]			
	$WW_h + ZZ_h$	$\mathcal{O}(\alpha)$	$\mathcal{O}(\alpha_s)$	all
SPS1a	-0.329	-0.469	-0.015	-0.484
SPS1b	-0.162	-0.229	-0.006	-0.235
SPS2	-0.147	0.129	-0.002	-0.131
SPS3	-0.146	-0.216	-0.006	-0.222
SPS4	-0.258	-0.355	-0.008	-0.363
SPS5	-0.606	-0.912	-0.010	-0.922
SPS6	-0.226	-0.309	-0.010	-0.319
SPS7	-0.206	-0.317	-0.006	-0.323
SPS8	-0.157	-0.206	-0.004	-0.210
SPS9	-0.094	-0.071	-0.003	-0.074

Table IV: Complete MSSM corrections for all SPS parameter points [21]. The vertex correction in the first column corresponds to Tab.II, but including all partonic channels.

corrections sharply drop with increasing  $m_{1/2}$ , as we approach the decoupling limit. Fixing  $\mu$  means larger corrections for a light SUSY spectrum and a sharper drop for heavy masses. The maximum size for the corrections consistent with the LEP2 chargino limit we read off to be  $-2\%$ . If we tune all weak-scale MSSM parameters to barely respect all LEP2 and Tevatron limits we find that the size of the supersymmetric corrections is bounded by  $-4\%$ . Explicit non-decoupling effects in the bottom Yukawa only appear in this process at the two-loop level, which means all curves in Fig. 2 decouple smoothly for increasing masses. Consistent with our previous discussion the  $\mathcal{O}(\alpha_s)$  corrections are negligible over the entire parameter range.

**Outlook** — In the light of a possible precision analysis of the Standard-Model and MSSM Higgs sector at the LHC we have analyzed the size of the supersymmetric one-loop corrections to the weak-boson-fusion production process  $qq \rightarrow qgh$ .

The appearance of all supersymmetric neutral Higgs bosons in the loops required us to study the impact of different methods of describing higher-order effects on Higgs masses and the Higgs potential. We find that the corrections from the Higgs sector are at the per-cent level, with a remaining uncertainty of below  $0.1\%$  due to these calculational approaches — simply reflecting unknown higher-order corrections.

The supersymmetric one-loop QCD corrections are not only suppressed to a typical NNLO level, but turn out to be negligible. This is due to a variety of effects, based on the color structure, the supersymmetric coupling structure, or the kinematics of the process. The complete set of electroweak loop diagrams contributes at the per-cent level, as is expected for massive  $\mathcal{O}(\alpha)$  corrections.

In total, the supersymmetric one-loop corrections to Higgs production via vector-boson fusion can be up to  $4\%$  for parameter points allowed by direct SUSY searches and are typically at or below  $1\%$ . Their sign is in general negative. This result should serve as a solid basis for a

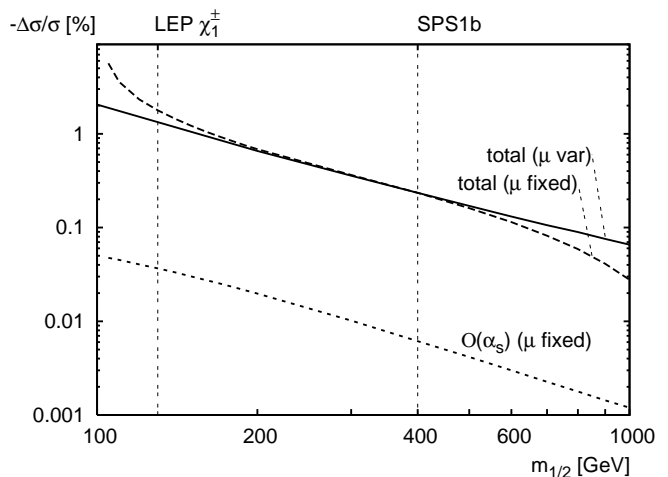


Figure 2: Relative next-to-leading order corrections as a function of  $m_{1/2}$  for varying and for fixed  $\mu$ . For the latter we show the strong corrections independently. The vertical lines indicate the chargino mass limit from LEP2 and the reference point SPS1b.

precision analysis of the supersymmetric Higgs sector at the LHC.

**Acknowledgments** — We would like to thank Dominik Stöckinger and Thomas Binoth for valuable discussions. We would also like to thank the PhenoGrid VO and ScotGrid for providing computer resources. This work was supported in part by the European Community’s Marie-Curie Research Training Network under contract MRTN-CT-2006-035505 ‘Tools and Precision Calculations for Physics Discoveries at Colliders’ (HEPTOOLS).

- 
- [1] S. Asai *et al.*, Eur. Phys. J. C **32S2**, 19 (2004).
  - [2] D. L. Rainwater, D. Zeppenfeld and K. Hagiwara, Phys. Rev. D **59**, 014037 (1999); T. Plehn, D. L. Rainwater and D. Zeppenfeld, Phys. Rev. D **61**, 093005 (2000).
  - [3] T. Plehn, D. L. Rainwater and D. Zeppenfeld, Phys. Lett. B **454**, 297 (1999).
  - [4] M. Dührssen *et al.*, Phys. Rev. D **70**, 113009 (2004).
  - [5] A. Djouadi, Phys. Rept. **457**, 1 (2008) and Phys. Rept. **459**, 1 (2008).
  - [6] T. Han, G. Valencia and S. Willenbrock, Phys. Rev. Lett. **69**, 3274 (1992); M. Spira, Fortsch. Phys. **46**, 203 (1998); T. Figy, C. Oleari and D. Zeppenfeld, Phys. Rev. D **68**, 073005 (2003); M. Ciccolini, A. Denner and S. Dittmaier, Phys. Rev. Lett. **99**, 161803 (2007).
  - [7] J. R. Andersen, T. Binoth, G. Heinrich and J. M. Smillie, JHEP **0802**, 057 (2008); A. Bredenstein, K. Hagiwara and B. Jäger, arXiv:0801.4231 [hep-ph].
  - [8] P. Bechtle, K. Desch, W. Porod and P. Wienemann, Eur. Phys. J. C **46**, 533 (2006); R. Lafaye, T. Plehn, M. Rauch and D. Zerwas, arXiv:0709.3985 [hep-ph].
  - [9] A. Djouadi and M. Spira, Phys. Rev. D **62**, 014004 (2000); M. Mühlleitner and M. Spira, Nucl. Phys. B **790**, 1 (2008); C. Anastasiou, S. Beerli and A. Daleo,

- arXiv:0803.3065 [hep-ph].
- [10] M. Rauch, arXiv:0804.2428 [hep-ph].
- [11] T. Hahn, *Comput. Phys. Commun.* **140**, 418 (2001); T. Hahn and C. Schappacher, *Comput. Phys. Commun.* **143**, 54 (2002); T. Hahn and M. Perez-Victoria, *Comput. Phys. Commun.* **118**, 153 (1999).
- [12] T. Hahn and M. Rauch, *Nucl. Phys. Proc. Suppl.* **157**, 236 (2006); A. Denner and S. Dittmaier, *Nucl. Phys. B* **658**, 175 (2003).
- [13] see e.g. S. Dittmaier, G. Hiller, T. Plehn and M. Spannowsky, arXiv:0708.0940 [hep-ph].
- [14] P. H. Chankowski, S. Pokorski and J. Rosiek, *Nucl. Phys. B* **423**, 437 (1994); R. Hempfling and A. H. Hoang, *Phys. Lett. B* **331**, 99 (1994); D. M. Pierce, J. A. Bagger, K. T. Matchev and R. J. Zhang, *Nucl. Phys. B* **491**, 3 (1997); S. Heinemeyer, W. Hollik and G. Weiglein, *Phys. Rev. D* **58**, 091701 (1998); R. J. Zhang, *Phys. Lett. B* **447**, 89 (1999); J. R. Espinosa and R. J. Zhang, *JHEP* **0003**, 026 (2000) and *Nucl. Phys. B* **586**, 3 (2000).
- [15] M. Frank, H. Rzehak *et al.*, *JHEP* **0702**, 047 (2007).
- [16] H. E. Haber and R. Hempfling, *Phys. Rev. D* **48**, 4280 (1993); J. A. Casas, J. R. Espinosa, M. Quiros and A. Riotto, *Nucl. Phys. B* **436**, 3 (1995) [Erratum-ibid. B **439**, 466 (1995)]; M. S. Carena, M. Quiros and C. E. M. Wagner, *Nucl. Phys. B* **461**, 407 (1996); H. E. Haber, R. Hempfling and A. H. Hoang, *Z. Phys. C* **75**, 539 (1997); S. P. Martin, *Phys. Rev. D* **66**, 096001 (2002) and *Phys. Rev. D* **71**, 016012 (2005).
- [17] M. S. Carena, J. R. Espinosa, M. Quiros and C. E. M. Wagner, *Phys. Lett. B* **355**, 209 (1995).
- [18] M. S. Carena, H. E. Haber, S. Heinemeyer, W. Hollik, C. E. M. Wagner and G. Weiglein, *Nucl. Phys. B* **580**, 29 (2000); G. Degrassi, S. Heinemeyer, W. Hollik, P. Slavich and G. Weiglein, *Eur. Phys. J. C* **28**, 133 (2003).
- [19] A. Sirlin and R. Zucchini, *Nucl. Phys. B* **266**, 389 (1986).
- [20] W. Hollik and S. Penaranda, *Eur. Phys. J. C* **23**, 163 (2002); A. Dobado, M. J. Herrero, W. Hollik and S. Penaranda, *Phys. Rev. D* **66**, 095016 (2002).
- [21] B. C. Allanach *et al.*, in *Proc. Snowmass 2001* [arXiv:hep-ph/0202233].